Facile Bond-forming and -breaking Process at Phosphorus, Carbon, and Oxygen Centres in Tungsten–Cobalt Complexes: *X*-Ray Crystal Structures of $[WCo(OH)(\mu-CC_6H_4Me-4)(\mu-PPh_2)_2(CO)_2(\eta-C_5H_5)]$, $[WCo(O)\{\mu-C(C_6H_4Me-4)C(O)\}(\mu-PPh_2)(CO)(PPh_2H)(\eta-C_5H_5)]$, and the Novel Alkyne Complex $[WCo(O)\{\mu-C(C_6H_4Me-4)C(OMe)\}(\mu-PPh_2)(CO)(PPh_2H)(\eta-C_5H_5)][BF_4]$

El Amin E. El Amin, John C. Jeffery,* and Tracy M. Walters

Department of Inorganic Chemistry, The University of Bristol, Bristol BS8 1TS, U.K.

Treatment of the complex $[WCo_2(\mu_3-CC_6H_4Me-4)(CO)_8(\eta-C_5H_5)]$ with an excess of PPh_2Cl results in cluster fragmentation and formation of the dimetal complex $[WCo(Cl)(\mu-CC_6H_4Me-4)(\mu-PPh_2)_2(CO)_2(\eta-C_5H_5)]$ which is an important precursor to a range of related W–Co derivatives; the structures of the complexes $[WCo(OH)(\mu-CC_6H_4Me-4)(\mu-PPh_2)_2(CO)_2(\eta-C_5H_5)]$, $[WCo(O)\{\mu-C(C_6H_4Me-4)C(O)\}(\mu-PPh_2)(CO)(PPh_2H)(\eta-C_5H_5)]$, and $[WCo(O)\{\mu-C(C_6H_4Me-4)C(OMe)\}(\mu-PPh_2)(CO)(PPh_2H)(\eta-C_5H_5)][BF_4]$ have been determined by *X*-ray diffraction and the latter complex exhibits an unusual alkyne bonding mode.

We have previously reported that treatment of the complexes $[MCo_2(\mu_3-CC_6H_4Me-4)(CO)_8(\eta-C_5H_5)]$ [M = W (**1**) or Mo][1] or $[WFe_2(\mu_3-CC_6H_4Me-4)(\mu-CO)(CO)_8(\eta-C_5H_5)]$[2] with secondary phosphine ligands provides an efficient route for the synthesis of trimetal complexes with bridging $\mu-PR_2$ and hydride ligands. We have now extended this approach to include the reactions of PPh_2Cl in the hope of obtaining related heterotrimetal complexes with chloride ligands replacing the hydride ligands. In fact, the reaction of (**1**) with PPh_2Cl affords a dimetal chloro-complex which is a precursor to a range of novel hydroxy and oxo W–Co dimetal species.

Treatment of the heterotrimetal complex (**1**) with an excess (3 equivs.) of PPh_2Cl (CH_2Cl_2, 42 °C) causes cluster fragmentation and following chromatography on dry alumina, moderate yields (*ca.* 50%) of the bright yellow dimetal complex $[WCo(Cl)(\mu-CC_6H_4Me-4)(\mu-PPh_2)_2(CO)_2(\eta-C_5H_5)]$ (**2**) were isolated (Scheme 1). Compound (**2**) is very sensitive to hydrolysis and if the former reaction mixture is chromatographed on deactivated alumina the related orange hydroxy derivative $[WCo(OH)(\mu-CC_6H_4Me-4)(\mu-PPh_2)_2(CO)_2(\eta-C_5H_5)]$ (**3**) is obtained in similar yields. The structure of (**3**) was established by a single crystal *X*-ray diffraction study[†] (Figure 1) which shows a W–Co dimetal alkylidyne complex with two symmetrically disposed $\mu-PPh_2$ ligands and a hydroxy ligand attached to the W atom. Spectroscopic data[‡] for (**2**) and (**3**) are very similar and are consistent with the solid state structure established for (**3**). In the ^1H NMR spectra, steric crowding about the W–Co bond leads to unusually shielded chemical shifts for the *ortho*-protons of the C_6H_4Me-4 ligand which are constrained to lie in the face of phenyl rings of the $\mu-PPh_2$ ligands.

In solution the hydroxy complex (**3**) slowly (10 h, 20 °C) isomerises to the sterically less crowded oxo complex $[WCo(O)\{\mu-C(C_6H_4Me-4)C(O)\}(\mu-PPh_2)(CO)(PPh_2H)(\eta-$

[†] *Crystal data* for (**3**): $C_{39}H_{33}CoO_3P_2W$, $M = 854.4$, monoclinic, space group $P2_1/c$ (no. 14), $a = 20.878(3)$, $b = 9.045(2)$, $c = 20.715(3)$ Å, $\beta = 116.98(2)°$, $U = 3486(1)$ Å^3, $Z = 4$, $D_c = 1.63$ g cm^{-3}, $F(000) = 1688$, $\mu(Mo-K_\alpha) = 40.3$ cm^{-1}, $R = 0.037$ ($R_w = 0.038$) for 4499 unique absorption corrected intensities [298 K, ω-scans, $2\theta \leqslant 50°$, $F \geqslant 5\sigma(F)$, Mo-K_α ($\bar{\lambda} = 0.71069$ Å)]. For (**4**): $C_{39}H_{33}CoO_3P_2W$, $M = 854.4$, orthorhombic, space group $P2_1nb$ (non-standard setting of $Pna2_1$ no. 33), $a = 10.648(1)$, $b = 20.107(3)$, $c = 16.036(2)$ Å, $U = 3433.1(7)$ Å^3, $Z = 4$, $D_c = 1.65$ g cm^{-3}, $F(000) = 1688$, μ(Mo-K$_\alpha$) = 40.3 cm^{-1}, $R = 0.026$ ($R_w = 0.027$) for 2925 unique absorption corrected intensities [298 K, θ—2θ scans, $2\theta \leqslant 50°$, $F \geqslant 4\sigma(F)$, Mo-K_α ($\bar{\lambda} = 0.710\ 69$ Å)]. For (**8a**)·(1/2CH_2Cl_2)·(1/2Et_2O): $C_{40}H_{36}BCoF_4O_3P_2W$·(1/2$CH_2Cl_2$)·(1/2$Et_2O$), $M = 1035.8$, monoclinic, space group $I2/a$ (non-standard setting of space group $C2/c$ no. 15), $a = 12.282(4)$, $b = 17.918(5)$, $c = 39.497(8)$ Å, $\beta = 89.95(2)°$, $U = 8671(4)$ Å^3, $Z = 8$, $D_c = 1.59$ g cm^{-3}, $F(000) = 4112$, μ(Mo=K$_\alpha$) = 32.8 cm^{-1}, $R = 0.041$ ($R_w = 0.044$) for 4190 unique absorption corrected intensities [298 K, WycKoff ω-scans, $2\theta \leqslant 45°$, $F \geqslant 5\sigma(F)$, Mo-K_α ($\bar{\lambda} = 0.710\,69$ Å)]. Data were collected on Nicolet P3 or P2$_1$ diffractometers and the structures were solved by heavy atom and difference-Fourier methods. The structures were refined by blocked-cascade or full-matrix least-squares procedures using the SHELX system of programs. Atomic co-ordinates, bond lengths and angles, and thermal parameters have been deposited at the Cambridge Crystallographic Data Centre. See Notice to Authors, Issue No. 1.

[‡] All compounds have been fully characterised by elemental analysis and spectroscopy. Only selected spectroscopic data are given. Unless otherwise noted IR spectra were measured in CH_2Cl_2 and NMR spectra in CD_2Cl_2 or CH_2Cl_2–CD_2Cl_2. Coupling constants in Hz, chemical shifts in p.p.m. relative to $SiMe_4$ [^1H, $^{13}C\{^1H\}$] or external H_3PO_4 [$^{31}P\{^1H\}$]. Compound (**2**): yellow crystals, $\nu_{max.}$ (CO) at 2020 s and 1976 s cm^{-1}; NMR: ^1H, δ 4.86 [d, 2 H, C(2) and C(6) of C_6H_4Me-4, *J*(HH) 8]; $^{31}P\{^1H\}$, δ 79.4 ($\mu-PPh_2$); $^{13}C\{^1H\}$, δ 335.3 [t, μ-*C*R, *J*(PC) 51], 210.0, 207.2 (2 × s, br., CoCO). Compound (**3**): orange crystals, $\nu_{max.}$ (CO) at 2010 s and 1967 s cm^{-1}; NMR: ^1H, δ 4.83 [d, 2 H, C(2) and C(6) of C_6H_4Me-4, *J*(HH) 8]; $^{31}P\{^1H\}$, δ 93.7 ($\mu-PPh_2$); $^{13}C\{^1H\}$, δ 326.0 [t, μ-*C*R, *J*(PC) 51], 210.5 (br., CoCO), 208.4 [t, CoCO, *J*(PC) 11]. Compound (**4**): dark-red crystals, $\nu_{max.}$ (CO) at 1958 s and 1714 m cm^{-1}; NMR: ^1H, δ 5.53 [d, 1 H, PPh_2H, *J*(PH) 291]; $^{31}P\{^1H\}$, δ 186.5 (br., $\mu-PPh_2$), 46.4 (br., PPh_2H); $^{13}C\{^1H\}$, δ 219.3 [d, μ-CR*C*(O), *J*(PC) 5], 218.1 (br., CoCO), 142.3—127.8 [μ-*C*(R)C(O), C_6H_5, C_6H_4]. Compound (**5**): yellow crystals, $\nu_{max.}$ (CO) at 2032 s and 1995 s cm^{-1}; NMR: ^1H, δ 4.93 [d, 2 H, C(2) and C(6) of C_6H_4Me-4, *J*(HH) 8]; $^{31}P\{^1H\}$, δ 84.8 ($\mu-PPh_2$); $^{13}C\{^1H\}$, δ 336.8 [t, μ-*C*R, *J*(PC) 51], 208.7 (br., CoCO), 205.8 [t, CoCO, *J*(PC) 12]. Compound (**6**): red crystals, $\nu_{max.}$ (CO) at 2058 s, 2026 s, and 1937 m cm^{-1}: NMR: $^{31}P\{^1H\}$, δ 167.5 (br., $\mu-PPh_2$), −5.9 [br., $\mu-C(R)PPh_2$]; $^{13}C\{^1H\}$, δ 231.7 [WCO, *J*(WC) 153], 199.1, 196.3 (2 × s, br., CoCO), 145.0—122.9 [μ-*C*(R)PPh_2, C_6H_5, C_6H_4]. Compound (**7**): orange crystals, $\nu_{max.}$(CO) at 2028 s and 1978 s cm^{-1}; NMR: $^{31}P\{^1H\}$, δ 99.2 [d, $\mu-PPh_2$, *J*(PP) 88], 36.7 [d, PPh_2H, *J*(PP) 88]; $^{13}C\{^1H\}$, δ 343.7 [dd, μ-*CR*, *J*(PC) 17, 15], 209.8 [dd, CoCO, *J*(PC) 12, 12], 198.7 [dd, CoCO, *J*(PC) 15, 15]. Compound (**8a**): orange crystals, $\nu_{max.}$(CO) at 2000 s cm^{-1}; NMR: ^1H, δ 2.29 (s, 3 H, Me-4), 4.57 (s, 3 H, OMe); $^{31}P\{^1H\}$, δ 221.5 (br., $\mu-PPh_2$), 47.8 (br., PPh_2H); $^{13}C\{^1H\}$, δ 239.3 [d, μ-CR*C*(OMe), *J*(PC) 29], 214.4 [d, CoCO, *J*(PC) 12], 139.6—126.6 [μ-*C*(R)C(OMe), C_6H_5, C_6H_4], 68.0 (OMe), 21.4 (Me-4). Compound (**8b**): orange crystals, $\nu_{max.}$(CO) at 2000 s cm^{-1}; NMR: ^1H, δ 2.52 (s, 3 H, Me-4), 4.09 (s, 3 H, OMe); $^{31}P\{^1H\}$, δ 195.2 (br., $\mu-PPh_2$), 41.8 (br., PPh_2H); $^{13}C\{^1H\}$, δ 220.6 [d, μ-CR*C*(OMe), *J*(PC) 12], 204.7 [d, CoCO, *J*(PC) 12], 139.6—126.6 [μ-*C*(R)C(OMe), C_6H_5, C_6H_4], 68.8 (OMe), 21.2 (Me-4). Compound (**9**): red crystals, $\nu_{max.}$(CO) at 1909 s cm^{-1}; NMR: ^1H, δ 2.39 (s, 3 H, Me-4), 3.08 (s, 3 H, OMe); $^{31}P\{^1H\}$, δ 189.9 (br., $\mu-PPh_2$), 27.1 [br., μ-C(R)C(OMe)PPh_2]; $^{13}C\{^1H\}$, δ 214.1 (br., CoCO), 189.7 [d, μ-C(R)*C*(OMe)PPh_2, *J*(PC) 42], 150.6—124.3 [μ-*C*(R)C(OMe)PPh_2, C_6H_5, C_6H_4], 60.9 (OMe), 21.1 (Me-4).

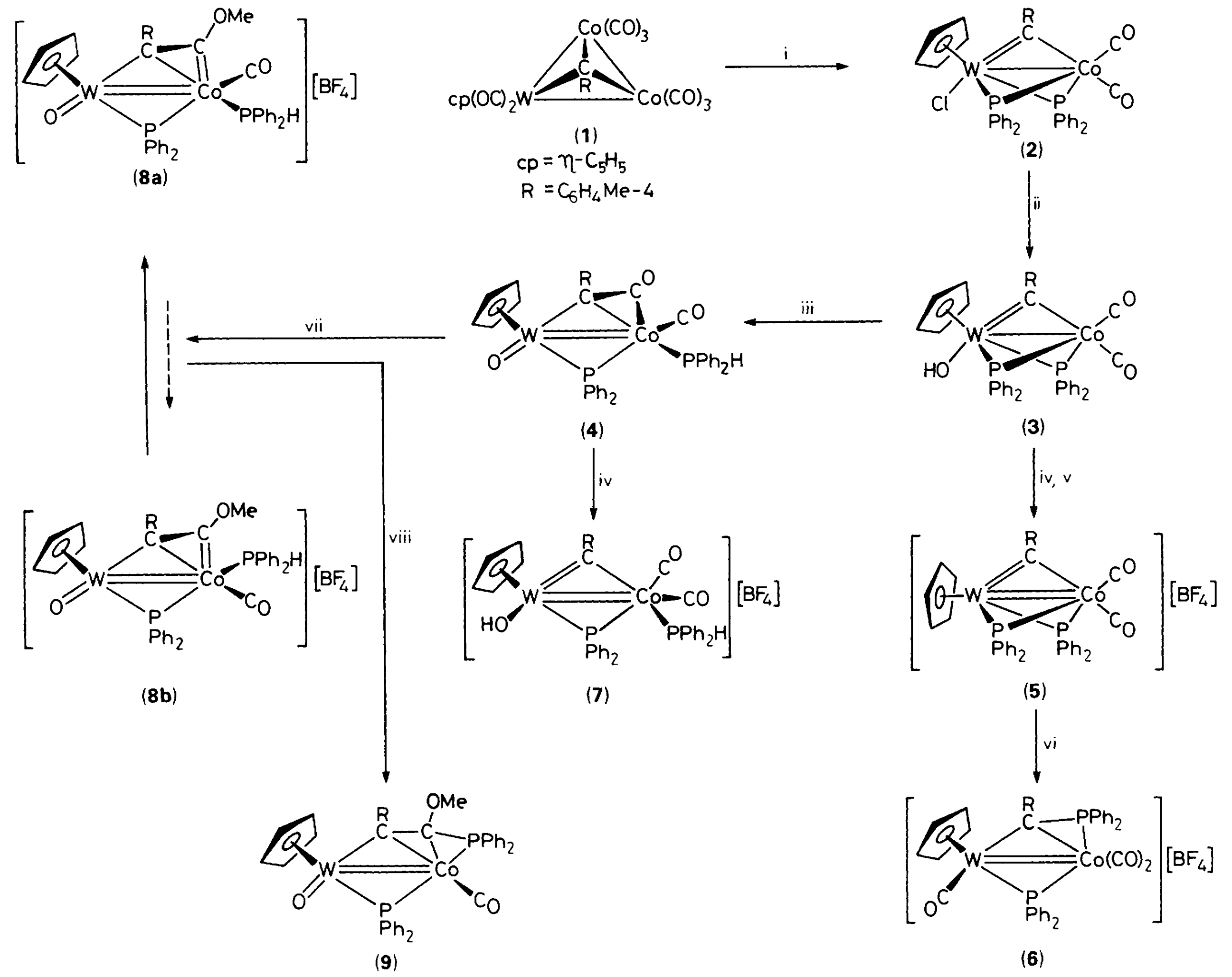

Scheme 1. i, PPh_2Cl, 42 °C, $-CoClL_n$; ii, deactivated alumina; iii, 10 h, 20 °C; iv, $HBF_4 \cdot Et_2O$; v, $-H_2O$; vi, $+CO$; vii, Me_3OBF_4; viii, base.

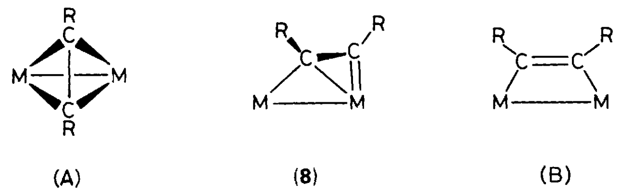

Scheme 2

$C_5H_5)]$ (**4**). Formation of (**4**) involves migration of a hydrogen atom from the hydroxy ligand to a μ-PPh_2 group, together with coupling of a CO ligand and the μ-CR group to give a bridging ketenyl {μ-C(R)C(O)} moiety. The structure of (**4**) was confirmed by a single crystal *X*-ray diffraction study (Figure 2).† The W–Co [2.584(1) Å] and W–O [1.709(6) Å] separations in (**4**) are shorter than found in the precursor (**3**) [W–Co 2.594(1) and W–OH 2.087(6) Å] which is consistent with the presence of appreciable W=Co and W=O multiple bond character.

Protonation of the complex (**3**) (CH_2Cl_2, $HBF_4 \cdot Et_2O$) occurs at the hydroxy ligand leading to loss of H_2O and formation of the symmetric co-ordinatively unsaturated cation $[WCo(\mu\text{-}CC_6H_4Me\text{-}4)(\mu\text{-}PPh_2)_2(CO)_2(\eta\text{-}C_5H_5)][BF_4]$ (**5**). Apart from appropriate chemical shift changes, NMR spectroscopic data for (**5**) are similar to those of the parent complex (**3**).‡ Treatment of (**5**) with CO promotes coupling of the μ-CR ligand with one of the μ-PPh_2 groups, quantitatively affording the μ-C(R)PPh_2 derivative $[WCo\{\mu\text{-}C(C_6H_4Me\text{-}4)PPh_2\}(\mu\text{-}PPh_2)(CO)_3(\eta\text{-}C_5H_5)][BF_4]$ (**6**), a rare example of a complex with a phospha-alkyne ligand bridging a dimetal centre.[3]

Protonation of the isomeric, co-ordinatively unsaturated complex (**4**) (CH_2Cl_2, $HBF_4 \cdot Et_2O$) occurs at the oxo ligand and the resulting loss of electron density at W promotes cleavage of the μ-C(R)–C(O) bond affording the hydroxy-alkylidyne cation $[WCo(OH)(\mu\text{-}CC_6H_4Me\text{-}4)(\mu\text{-}PPh_2)(CO)_2(PPh_2H)(\eta\text{-}C_5H_5)][BF_4]$ (**7**). The presence of the μ-CR ligand in (**7**) was readily established by the observation of a characteristic signal for the μ-CR ligand at δ 343.7 [dd, μ-*C*R, *J*(PC) 17, 15 Hz]. The complex (**7**) shows no tendency to lose H_2O to form (**5**) and unlike the latter complex does not react with CO.

In marked contrast, methylation (Me_3OBF_4) of (**4**) occurs at the oxygen centre of the μ-C(R)C(O) ligand leading to the formation of the methoxy-alkyne complex $[WCo(O)\{\mu\text{-}C(C_6H_4Me\text{-}4)C(OMe)\}(\mu\text{-}PPh_2)(CO)(PPh_2H)(\eta\text{-}C_5H_5)][BF_4]$ (**8**). In solution, NMR spectroscopic data show that (**8**) exists as a mixture of two isomers [(**8a**) : (**8b**) 4 : 1] which slowly interconvert on the NMR time scale. A single crystal *X*-ray diffraction study shows that isomer (**8a**) is favoured in the solid

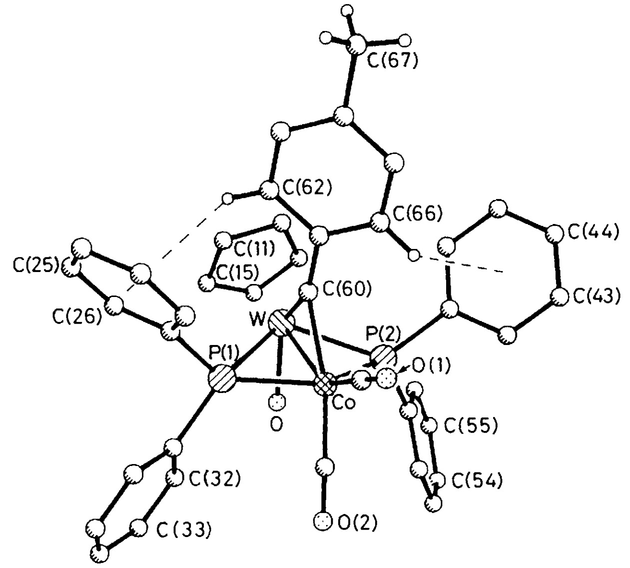

Figure 1. Molecular structure of $[WCo(OH)(\mu\text{-}CC_6H_4Me\text{-}4)(\mu\text{-}PPh_2)_2(CO)_2(\eta\text{-}C_5H_5)]$ (**3**). Bond lengths and angles: W–Co 2.594(1), W–P(1) 2.423(2), W–P(2) 2.417(2), W–O 2.087(6), W–C(60) 1.936(8), Co–P(1) 2.210(2), Co–P(2) 2.212(2), Co–C(60) 2.001(7) Å; Co–W–C(60) 49.9(2), W–Co–C(60) 47.7(2), W–C(60)–Co 82.4(3), W–P(1)–Co 67.9(1), W–P(2)–Co 68.0(1)°.

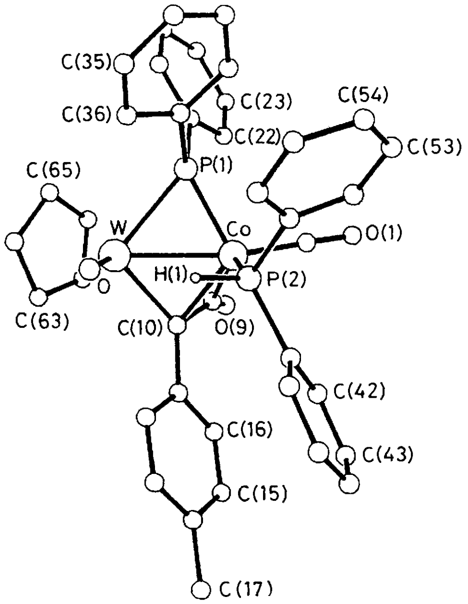

Figure 2. Molecular structure of $[WCo(O)\{\mu\text{-}C(C_6H_4Me\text{-}4)C(O)\}(\mu\text{-}PPh_2)(CO)(PPh_2H)(\eta\text{-}C_5H_5)]$ (**4**). Bond lengths and angles: W–Co 2.584(1), W–P(1) 2.427(2), W–O 1.709(6), W–C(10) 2.101(6), Co–P(1) 2.125(2), Co–P(2) 2.231(2), Co–C(10) 2.026(6), Co–C(9) 1.922(6), C(9)–C(10) 1.39(1), P(2)–H(1) 1.27(6) Å; Co–W–C(10) 50.0(2), W–Co–C(10) 52.5(2), W–C(10)–Co 77.5(2), W–P(1)–Co 68.8(1)°.

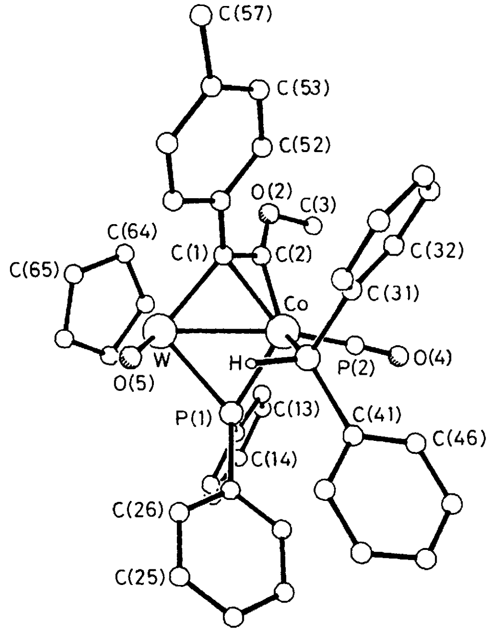

Figure 3. Molecular structure of $[WCo(O)\{\mu\text{-}C(C_6H_4Me\text{-}4)C(OMe)\}(\mu\text{-}PPh_2)(CO)(PPh_2H)(\eta\text{-}C_5H_5)][BF_4]$ (**8a**). Bond lengths and angles: W–Co 2.612(1), W–P(1) 2.410(2), W–O(5) 1.710(6), W–C(1) 2.108(9), W···C(2) 2.764, Co–P(1) 2.153(3), Co–P(2) 2.209(3), Co–C(1) 2.057(9), Co–C(2) 1.806(9) Å; Co–W–C(1) 50.3(2), W–Co–C(1) 52.0(3), W–C(1)–Co 77.7(3), W–P(1)–Co 69.6(1), W–C(1)–Co 77.7(3), W–C(1)–C(2) 103.3(6), Co–C(1)–C(2) 59.7(5), W–C(1)–C(51) 129.7(6), Co–C(1)–C(51) 134.6(6), C(2)–C(1)–C(51) 125.6(8), Co–C(2)–C(1) 79.5(6), Co–C(2)–O(2) 150.8(8), C(1)–C(2)–O(2) 129.4(9)°. The position of the P(2)–H hydrogen atom was obtained from a final electron density difference synthesis but was not refined.

state (Figure 3).† The alkyne adopts an extremely novel bonding mode. The ligated carbon atom carrying the tolyl substituent bridges the W–Co bond [W–C(1) 2.108(9) and Co–C(1) 2.057(9) Å] whilst the methoxy substituted end of the alkyne is bound only to the Co metal centre [Co–C(2) 1.806(9) and W···C(2) 2.764 Å]. The resulting bonding mode is thus intermediate between the well established transverse (A) and in-plane (B) alkyne bonding modes shown in Scheme 2.

Deprotonation (NaOMe–MeOH) of the mixture of isomers (**8a,b**) proceeds smoothly, affording the neutral complex $[WCo(O)\{\mu\text{-}C(C_6H_4Me\text{-}4)C(OMe)PPh_2\}(\mu\text{-}PPh_2)(CO)(\eta\text{-}C_5H_5)]$ (**9**). Spectroscopic data for (**9**) suggest a structure in which the alkyne ligand and a PPh_2 moiety have coupled to form a $\mu\text{-}C(C_6H_4Me\text{-}4)C(OMe)PPh_2$ group.

These studies demonstrate that fundamental P–C and C–C bond making and breaking reactions can occur under extremely mild conditions at W–Co dimetal centres.

We thank the University of Khartoum for a scholarship and the CVCP for an ORS award (El Amin).

Received, 4th October 1989; Com. 9/04260A

References

1 P. Dunn, J. C. Jeffery, and P. Sherwood, *J. Organomet. Chem.*, 1986, **311**, C55; M. R. Bradford, N. G. Connelly, N. C. Harrison, and J. C. Jeffery, *Organometallics*, 1989, **8**, 182.
2 J. C. Jeffery and J. G. Lawrence-Smith, *J. Chem. Soc., Chem. Commun.*, 1986, 17; *J. Chem. Soc., Dalton Trans.*, in the press.
3 S. J. Davies, J. A. K. Howard, M. U. Pilotti, and F. G. A. Stone, *J. Chem. Soc., Chem. Commun.*, 1989, 190.